A STUDY OF TYRE CAVITY RESONANCE AND ITS MITIGATION USING MODAL ANALYSIS METHOD

Napasin Chanpong[1]; Zamri Mohammad[1]; Haiqiao Wei[2], Simon Watkins[1], Xu Wang[1]

[1] RMIT University, Australia

[2] Tianjin University, P. R. China

ABSTRACT

This paper will focus on determining characteristics of tyre cavity resonance noise and its mitigation method. There are many factors that affect the noise transmitted to vehicle cabin, this includes coupling mode of structure and tyre air cavity which will be investigated in this paper. The results from experimental modal analysis will be compared with those from finite element modal analysis. These investigations would lead to understanding and reduction of tyre cavity resonance noise. Tyre samples were tested for their material properties using tensile tests and wheel assembly was tested for its dynamic properties through roving impact hammer tests. The frequency response data of roving impact hammer tests on a wheel tyre assembly was processed using MEScope software for identifying its mode shape. The results have shown the significant vibration response amplitude peak between 200-250 Hz is related to the tyre cavity resonance noise.

Keywords: Tyre cavity, resonance, modal analysis, tyre noise

1. INTRODUCTION

Most of vehicle noise comes from engine, wind and tyre. At present, advance NVH technology could eliminate engine noise and reduce its transmission to the cabin. Aerodynamic noise could be well insulated. Tyre noise became more important for automotive car makers than wind noise and engine noise because customer's requirement is a larger wheel with thinner side wall which has an adverse effect of the tyre noise (Nguyen & Wang, 2010). The tyre noise is greater than engine noise in modern car when it was driving above 40 km/hr (Kindt, et al., 2009). Rubber tyre, since it had been made, provided shock absorption to vehicle and developed contact surface to the ground; on the other hand, it generated the tyre noise heard inside cabin. There is an urgent need to develop the premium luxury car with advanced automotive technology that gives extremely comfortable driving experience. Especially, for an electrical car, petrol engine has been already removed from the car, therefore, the noise from the engine is eliminated. For electrical car, tyre noise and wind noise would play a major role. Noise performance plays a crucial role as noise induces hearing loss (NIHL). A long time exposure to a high level of noise could cause temporary threshold shift (TTS) and affect the hearing performance. Thus, the noise performance is related to not only the customer satisfaction, but also the occupational health and safety (Nguyen & Wang, 2010). Tyre cavity resonance noise significantly affects the perception of driving experience, the ability to concentrate and leads to increasing fatigue. A new method needs to be developed to reduce or eliminate the tyre cavity resonance noise.

There are tyre cavity mode, tyre structure mode and rim structure mode. Computational methods were most used to determine natural frequencies and mode shapes of tyre structure, tyre cavity, and rim structure. There were three interior noise frequency response function amplitude peaks corresponding to the tyre noise which could be seen between 60 to 400 Hz as shown in Figure 1. Two of them would be changed due to the tyre or rim structure or tyre pressure change. The frequency near 250 Hz was related to the cavity resonance noise (Sakata, et al., 1990).

[1] xu.wang@rmit.edu.au
[2] whq@tju.edu.cn

The other factors such as suspension design, the media filled in tyre, could lead to a difference in the transmitted noise level (Scavuzzo, et al., 1994). The energy balance model was developed to calculate tyre cavity resonance noise. Finite element analysis was used to estimate the frequency response of the tyre and rim under an excitation force.

For a simple calculation method to determine the resonance frequency of the noise, a 2-dimensional model is assumed where the tyre structure is cut and stretched to be straight. Then, the formula for the resonant frequency was given by

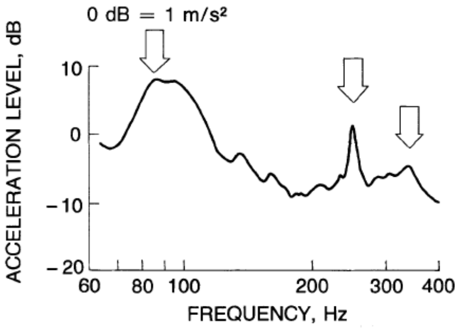

Figure 1 – This is a caption for the figure

$$f = \frac{c}{L} \tag{1}$$

where

f is the resonance frequency,

c is the speed of sound in the cavity medium

L is the circumference of tyre at the mean radius of the tyre cavity.

In addition, structural-acoustic coupling has generated high response amplitude at modal resonance frequencies of the structure and cavity which are close to each other. This high response amplitude causes greater sound pressure level transmitted to a cabin (Lau & Tang, 2003).

This paper will focus on a study of tyre cavity resonance noise to find possible mitigation methods which could be applied to reduce the cabin noise. Various factors that affect the vibration behavior and the tyre noise will be analyzed. Frequency response data of the tyre wheel assembly will be determined by both experimental and finite element analysis methods. The FEA data will be verified by experimental data. This research will explore solutions from reduction of structural-acoustic coupling of tyre and rim structures, and tyre cavity. Therefore, the research will benefit tyre and vehicle manufacturers and roads users.

2. TENSILE TEST FOR TYRE MATERIAL PROPERTIES

Tensile test was used to obtain material property data for ANSYS software input. Several pieces of tyre tread pattern were cut out in longitudinal and radial directions and tested. The sample sizes are listed in Tables 1-4. The experiments were divided into three groups where the specimens were tested under a pre-cyclic load, cyclic load and post-cyclic load at a speed of 50 mm/min for both extension and contraction. For pre-cyclic load and post-cyclic load, ultimate tensile strength (UTS), Elastic modulus and Poisson's ratio were measured. Moreover, cyclic load was used to pre-condition the tyre cut-out for ten cycles for a used tyre.

In order to measure Poisson's ratios of the cut-out samples, their width and width were measured before and after the extension. In order to calibrate the UTS test facility, the sizes of the samples were measured, and strain gauge was attached onto the samples for measuring strain under pre-cyclic and post-cyclic loads.

For pre-conditioning, tyre cut-outs were pulled 30 to 40 per cents of the maximum extension. The materials were extended without any separation inside materials. During each extension test, there were five minutes of a material relaxation time. These test load and extension displacement data were recorded. Maximum stresses, elastic modulus, and Poisson ratio were recorded from experimental tests and analyzed.

The experimental results were listed in Table 5 and Table 6.

Table 1 – Size of longitudinal direction tread pattern samples (all dimensions in mm).

	Tread
Original width	28.34
Original length	135
Original thickness with tread	16.12
Original thickness w/o tread	9.27

Table 2 – Size of longitudinal direction sidewall samples (all dimensions in mm).

	Tread
Original width	22.7
Original length	137.5
Original thickness with tread	7.7
Original thickness w/o tread	7.7

Table 3 – Size of radial direction tread pattern samples (all dimensions in mm).

	Tread
Original width	26.3
Original length	90
Original thickness with tread	16.6
Original thickness w/o tread	8.0

Table 4 – Size of radial direction sidewall samples (all dimension in mm).

	Tread
Original width	13.3
Original length	40
Original thickness with tread	7.2
Original thickness w/o tread	7.2

These structural properties of the tyre cut-out samples in both Tables 5 and 6 can be used when a force is applied in either the radial or longitudinal direction.

3. ROVING IMPACT TEST

In order to identify and analyse natural frequencies of tyre-rim assembly, frequency response function was measured from Fourier transform of the output response ($X(\omega)$) divided by that of the input force ($F(\omega)$) (Brian & Mark, 1999).

$$H(\omega) = \frac{X(\omega)}{F(\omega)} \tag{2}$$

Table 5 – Measured stresses and elastic modules of longitudinal cut-outs under pre- and post- cyclic loads.

Longitudinal cut-out		
Pre cyclic load	Tread	Sidewall
Maximum stress (MPa)	35.2	6.0
Elastic modulus (MPa)	290.8	1.8
Poisson ratio	0.4	0.2
Post cyclic load	Tread	Sidewall
Maximum Stress (MPa)	33.1	6.3
Elastic modulus (MPa)	246.3	1.5
Poisson ratio	0.4	0.3

Table 6 – Measured stresses and elastic modules of radial cut-outs under pre-cyclic and post-cyclic loads.

Radial cut-out		
Pre cyclic load	Tread	Sidewall
Maximum stress (MPa)	18.3	24.0
Elastic modulus (MPa)	170.5	197.0
Poisson ratio	0.2	0.2
Post cyclic load	Tread	Sidewall
Maximum Stress (MPa)	16.4	18.3
Elastic modulus (MPa)	150.5	111.7
Poisson ratio	0.3	0.2

In order to prepare the test, a tyre-rim assembly was marked with white dots at profile points and mounted on a stand. Output signals of accelerometer and force transducer of the impact hammer were connected to the frontend channels of a FFT analyzer and then connected to a computer through a data cable. The measurement data at each marked point was collected and analyzed in MEScope software. Three clear impacts were applied at each marked point, the frequency response functions were measured and averaged to identify the modal peak frequencies. In order to determine the modal resonance frequencies, frequency response function amplitude curves were plotted. Impact was first applied on tyre structure at white dot points as shown in Figure 2. These dot points were marked to divide the tyre circumference into 16 segments evenly, and there are two loops of dot points on the sidewall and 3 loops of dot points on the tread surface.

The measured frequency response function (FRF) data was imported into MEScope software to calculate the modal frequencies and mode shapes of the tyre-rim assembly. The impact test was then applied to a rim to identify natural frequencies of both aluminum alloy and steel rims. These experiments were performed for four different setting ups which were aluminum alloy rim assembled with tyre and mounted on a stand, aluminum alloy rim assembled with tyre and placed on a soft cushion, steel rim assembled with tyre and mounted on a stand and steel rim assembled with tyre and placed on a soft cushion. The soft cushion support was equivalent to a free support. The experiments were performed with a tyre pressure of 152.4 kPa.

Figure 2 – Tyre-rim assembly setup for roving impact tests

Experiment data has shown modal frequencies of a whole system as listed in Table 7. These modal frequencies identified by experiments will be compared with those calculated by finite element analysis and theoretical analysis. It is shown that the measured 7^{th} modal resonance frequency is 230 Hz. From the theoretical analysis in Equation (1), the calculated result was 227.6 Hz which means that the mode of steel rim could be coupled to the mode of the tyre cavity. Different modal frequencies and mode shapes can be calculated using the MEScope software.

Table 7 – Modal frequencies identified by MEScope.

Mode	Frequency (Hz)
1	59.2
2	81.7
3	88.2
4	130
5	142
6	220
7	230
8	241
9	326

As shown in Figure 3, the steel rim with free support doesn't have any modal peaks in the frequency range between 200 and 250 Hz. Therefore, the mode at 230 Hz for the steel rim mounted on a stand is related to mounting.

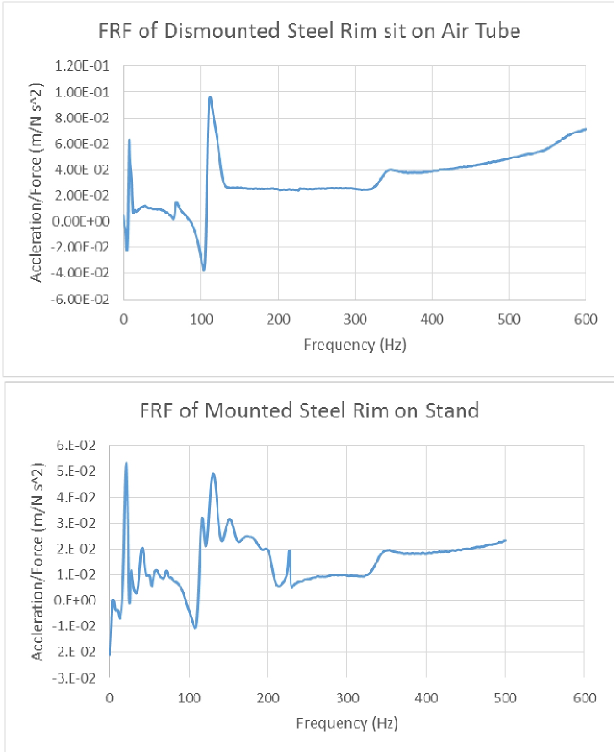

Figure 3 – Measured frequency response function amplitude curves of the tyre-rim assembly setup for roving impact tests

4. FINITE ELEMENT ANALYSIS AND DISCUSSIONS

4.1 Comparison of modal frequencies and mode shapes of the tyre-rim assembly from the ANSYS FEA simulations and roving impact tests

Finite element analysis was conducted where the properties of the tyre material were adopted from Tables 5 and 6, the properties of medium in tyre cavity, and rim material were imported into ANSYS software for further structural and acoustic simulations. Each of tyre structure, rim structure and tyre cavity was analyzed individually under different load and boundary conditions.

Modal frequencies and mode shapes were calculated and shown in Figure 4 where two identical modal frequencies appear, each of which corresponds to a mode shape due to the cavity geometric symmetry.

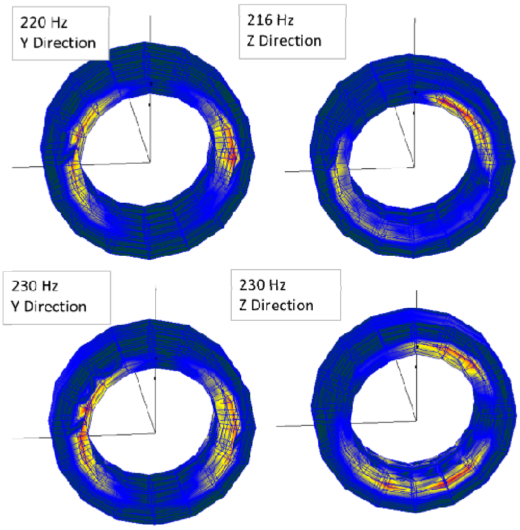

Figure 4 – Measured mode shapes of the tyre-rim assembly setup for roving impact tests

Mode 2: 226.12 Hz

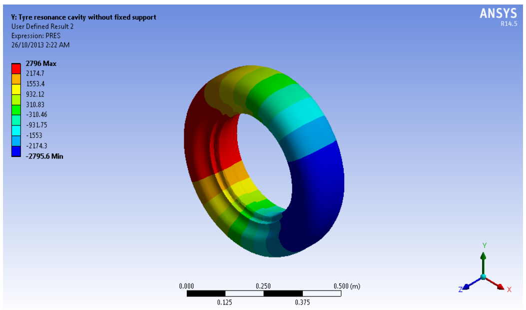

Mode 3: 226.14 Hz

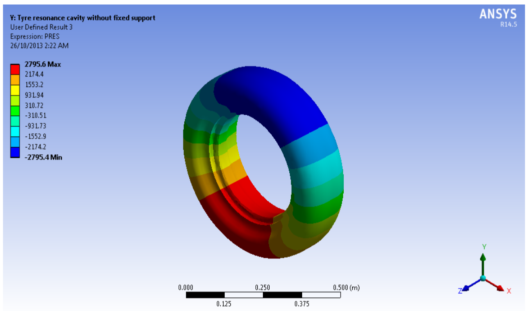

Figure 5 – Modal frequencies and mode shapes from ANSYS FEA simulation of the tyre-rim assembly setup

4.2 Tyre cavity

For the tyre cavity finite element analysis (FEA), the result for second and third modal resonant frequency is 226.1 Hz (as in Table 8 and Figure 5) which is close to 227.6 Hz calculated from Equation (1) where a sound speed of 343 m/s, 600 mm outer diameter, and 360 mm inner diameter are assumed. The resonant frequency results of air filled tyre cavity calculated by theoretical and finite element analyses are close to each other. From the ANASYS workbench analysis, the media filled inside tyre cavity such as air, nitrogen, and helium have different sound speeds which are presented in Table 9.

Table 8 – Tyre cavity resonant frequency for different filled media

Tyre Cavity	Resonance Frequency (Hz)		
	1st Mode	2nd Mode	3rd Mode
Air Filled	0	226.1	226.1
Nitrogen Filled	0	220.2	220.2
Helium Filled	0	636.2	636.2

Table 9 – Physical parameters of liquids

	Velocity (m/s)	Density (kg/m3)
Air	343	1.205
Nitrogen	334	1.165
Helium	965	0.1664

4.3 Tyre structure

According to the FEA, the natural frequencies of the tyre structure have been calculated with different tyre pressures and boundary conditions which are given in Table 10 where the old and new tyres were simulated for the first three natural frequencies with fixed and no fixed or free support and with 152.4 kPa tyre pressure applied onto the inner tyre surface. The tyre is a deflated one, the tyre pressure was set in random. The tyre size is Bridgestone 205/65/R15 RE92.

New tyre was the tyre which was purchased from a supplier and never used before. "Old" tyre was the tyre fitted into a vehicle which was driven for 20,000 km at least. For the fixed support, the bead cords were fixed or constrained in all directions. For no fixed or free support, zero frequency rigid body mode appears. If the rigid body mode is excluded, it is seen that the natural frequencies of the tyre with the fixed support are slightly larger than those with no fixed or free support. The natural frequencies of the new tyre are larger than those of the old tyre for the same boundary conditions. The modal frequency results with applied tyre pressure are much larger than those without applied tyre pressure. The tyre structure consists of three parts which are tread plate and two sidewalls as shown in Figure 6.

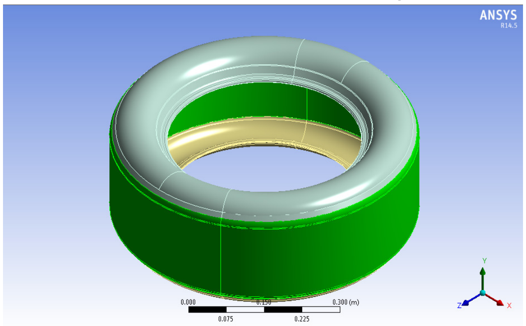

Figure 6 – Tyre structure with tread and two sidewalls

From the FEA workbench analysis, the tyre mode with modal frequency of 208.2 may couple with the tyre cavity resonant mode at 226.1 Hz for the brand new condition. However, the old tyre does not have such a mode which has a modal frequency close to that of the tyre cavity. The modal frequency of the old tyre is shifted down to 175.3 Hz. For no fixed boundary or free support, the FEA results will include a mode that has its modal frequency close to zero. As shown in Figure 7, the mode shape of the old tyre having free movement in X and Z-direction and no displacement in Y-direction, as it is called cylindrical support. It shows the seventh and eighth modes with modal frequencies of 250 Hz close to the tyre cavity resonant frequency of 226 Hz.

Mode 7: 249.93 Hz

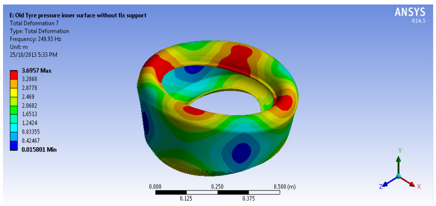

Mode 8: 250.3 Hz

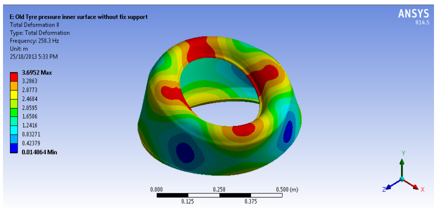

Figure 7 – Modal analysis of the old tyre with applied 152.4 kPa inner pressure applied and bottom displacement constrained in Y-direction.

4.4 Rim Model

FEA was conducted on the steel rim and aluminum alloy rim models as shown in Figure 8 and 9 where 3D geometry models were scanned and imported into ANSYS FEA workbench software applied with 152.4 kPa tyre pressure load and constraints at the edges of wheel hub and mounting bolt holes. The modal frequency results are presented in Table 11 for the steel rim and aluminum alloy rim with different boundary conditions. It is seen from Table 11 and Figure 3 that 231, 236 Hz are related to mounting modes as they change with boundary support conditions. The results of Table 11 have also been verified by those in Figure 3.

The results from FEA modal analysis of the steel rim show that the modal frequency of 231 Hz is very close to the calculated tyre cavity resonant frequency of 226.1 Hz by FEA, therefore, the tyre cavity resonant noise and vibration would be easily amplified and transmitted through the wheel hub into vehicle cabin.

The results from FEA modal analysis of aluminum alloy rim have shown that the modal frequency of 238 Hz is relatively far away from the FEA calculated tyre cavity resonance frequency of 226.1 Hz. There exists less modal coupling between the aluminum alloy rim and the tyre air cavity than between the steel rim and the tyre air cavity. Therefore, the aluminum alloy rim is better than the steel rim for reduction of the tyre resonance noise.

Table 10 – Modal analysis of tyre structure

		Frequency (Hz)		
Tyre tyres	Boundary conditions	6th Mode	7th Mode	8th Mode
Old tyre	152.4 kPa applied pressure onto the inner surface of the tyre with the cylindrical support	173.0	249.9	250.3
	152.4 kPa applied pressure onto the inner surface of the tyre with fixed support	175.3	306.6	306.8
New tyre	152.4 kPa applied pressure onto the inner surface of the tyre with fixed support	208.2	370.9	371.3
	152.4 kPa applied pressure onto the inner surface with cylindrical support	69.1	70.1	202.4

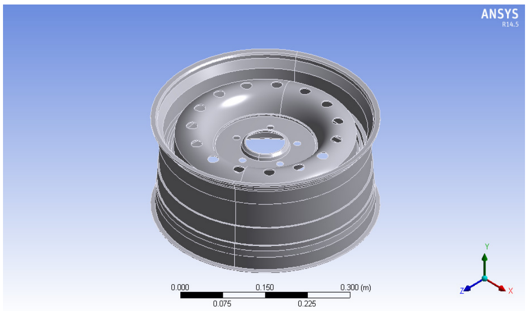

Figure 8– Steel rim model.

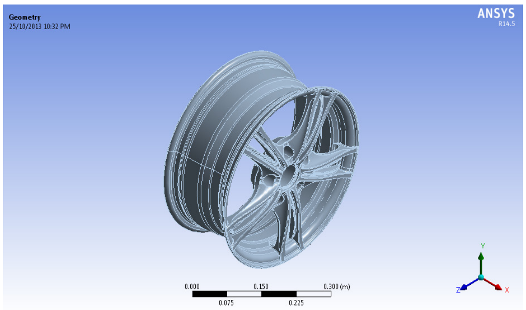

Figure 9– Aluminum alloy rim model.

Table 11 – Modal analysis of natural frequencies of steel rim model with different tyre pressure loads and constraints.

		Frequency (Hz)				
		1st Mode	2nd Mode	3rd Mode	4th Mode	5th Mode
Boundary conditions	steel rim mounted on a stand with fixed support at hub	112	114	236	413	508
	aluminum alloy rim mounted on a stand with fixed support at hub	113	115	238	410	509
	steel rim with tyre pressure applied on the surface and cylindrical support	28	28	63	231	231
	steel rim mounted on a stand with fixed support at hub	28	28	63	231	231

5. CONCLUSIONS

The steel rim has the resonance frequency close to the tyre cavity resonance frequency, which generates the modal coupling. As a result, the coupling mode of the tyre air cavity and the steel rim is significant which amplify the noise and vibration transmission. Therefore, the mitigation of the noise is to shift one of the two close modal frequencies of the rim and tyre air cavity such as by changing media in tyre cavity as the sound speed in media is directly proportional to the natural frequency or by changing shape of the rim model. The solution for shifting the resonance frequency of the rim is to design a rim model like that in Figure 8. The rim material change would change the natural frequency, but it does not shift its modal frequency far away from the cavity resonance frequency and does not eliminate the coupling mode.

ACKNOWLEDGEMENTS

A special thanks to Peter T from the RMIT NVH laboratory for helps in setting up experiments and Thierry P. E. for helping drawing aluminium alloy model.

REFERENCES

1. Brian, S. J. & Mark, R. H., 1999. *EXPERIMENTAL MODAL ANALYSIS*. Vibrant Technology, Inc.
2. Grecey & Associates, n.d. *Accoustic Glossary*. [Online] Available at: http://www.acoustic-glossary.co.uk/definitions-r.htm#reference [Accessed 10 April 2013].
3. Kindt, P. et al., 2009. Experimental analysis of the structure borne tyre/road noise due to road discontinuities. *Mechanical Systems and Signal Processing*, Volume 23, Issue 8, Pages 2557–2574.
4. Lau, S. & Tang, S., 2003. Impacts of structural-acoustic coupling on the performance of energy density-based active sound transmission control. *Journal of Sound and Vibration*, Volume 266, pp. 147-170.
5. Naerum, 1982. *Measuring Vibration*. Denmark: Bruel & Kjaer.
6. Sakata, T., Morimura, H. & Ide, H., 1990. Effects of Tyre Cavity Resonance on Vehicle Road Noise. *Tyre Science and Technology*, Volume 18, Issue 2, pp. 68-79.
7. Scavuzzo, W. R., Charek, T. L., Sandy, M. P. & Shtrinhauz, D. G., 1994. Influence of Wheel Resonance on Tyre Acoutic Cavity Noise. *SAE TECHNICAL PAPER 940533*.
8. Thompson, J. K., 1995. Plane Wave Resonance in the Tyre Air Cavity as a Vehicle Interior Noise Source. *Tyre Science and Technology*, Vol. 23, No. 1, pp. 2-10.
9. Mohamed, Z., Wang, X. and Jazar, R. (2013). 'A survey of wheel tyre cavity resonance noise', Vol. 9, Nos. 3/4, International Journal of Vehicle Noise and Vibration.